Bose–Einstein correlations of neutral and charged pions in hadronic Z decays

L3 Collaboration

P. Achard [t], O. Adriani [q], M. Aguilar-Benitez [x], J. Alcaraz [x,r], G. Alemanni [v], J. Allaby [r], A. Aloisio [ab], M.G. Alviggi [ab], H. Anderhub [au], V.P. Andreev [f,ag], F. Anselmo [i], A. Arefiev [aa], T. Azemoon [c], T. Aziz [j,r], M. Baarmand [y], P. Bagnaia [al], A. Bajo [x], G. Baksay [p], L. Baksay [y], S.V. Baldew [b], S. Banerjee [j], Sw. Banerjee [d], A. Barczyk [au,as], R. Barillère [r], P. Bartalini [v], M. Basile [i], N. Batalova [ar], R. Battiston [af], A. Bay [v], F. Becattini [q], U. Becker [n], F. Behner [au], L. Bellucci [q], R. Berbeco [c], J. Berdugo [x], P. Berges [n], B. Bertucci [af], B.L. Betev [au], M. Biasini [af], M. Biglietti [ab], A. Biland [au], J.J. Blaising [d], S.C. Blyth [ah], G.J. Bobbink [b], A. Böhm [a], L. Boldizsar [m], B. Borgia [al], S. Bottai [q], D. Bourilkov [au], M. Bourquin [t], S. Braccini [t], J.G. Branson [an], F. Brochu [d], A. Buijs [aq], J.D. Burger [n], W.J. Burger [af], X.D. Cai [n], M. Capell [n], G. Cara Romeo [i], G. Carlino [ab], A. Cartacci [q], J. Casaus [x], F. Cavallari [al], N. Cavallo [ai], C. Cecchi [af], M. Cerrada [x], M. Chamizo [t], Y.H. Chang [aw], M. Chemarin [w], A. Chen [aw], G. Chen [g], G.M. Chen [g], H.F. Chen [u], H.S. Chen [g], G. Chiefari [ab], L. Cifarelli [am], F. Cindolo [i], I. Clare [n], R. Clare [ak], G. Coignet [d], N. Colino [x], S. Costantini [al], B. de la Cruz [x], S. Cucciarelli [af], T.S. Dai [n], J.A. van Dalen [ad], R. de Asmundis [ab], P. Déglon [t], J. Debreczeni [m], A. Degré [d], K. Deiters [as], D. della Volpe [ab], E. Delmeire [t], P. Denes [aj], F. DeNotaristefani [al], A. De Salvo [au], M. Diemoz [al], M. Dierckxsens [b], D. van Dierendonck [b], C. Dionisi [al], M. Dittmar [au,r], A. Doria [ab], M.T. Dova [k,5], D. Duchesneau [d], P. Duinker [b], B. Echenard [t], A. Eline [r], H. El Mamouni [w], A. Engler [ah], F.J. Eppling [n], A. Ewers [a], P. Extermann [t], M.A. Falagan [x], S. Falciano [al], A. Favara [ae], J. Fay [w], O. Fedin [ag], M. Felcini [au], T. Ferguson [ah], H. Fesefeldt [a], E. Fiandrini [af], J.H. Field [t], F. Filthaut [ad], P.H. Fisher [n], W. Fisher [aj], I. Fisk [an], G. Forconi [n], K. Freudenreich [au], C. Furetta [z], Yu. Galaktionov [aa,n], S.N. Ganguli [j], P. Garcia-Abia [e,r], M. Gataullin [ae], S. Gentile [al], S. Giagu [al], Z.F. Gong [u], G. Grenier [w], O. Grimm [au], M.W. Gruenewald [h,a], M. Guida [am], R. van Gulik [b], V.K. Gupta [aj], A. Gurtu [j], L.J. Gutay [ar], D. Haas [e], D. Hatzifotiadou [i], T. Hebbeker [h,a], A. Hervé [r], J. Hirschfelder [ah], H. Hofer [au], G. Holzner [au], S.R. Hou [aw], Y. Hu [ad], B.N. Jin [g], L.W. Jones [c], P. de Jong [b],

I. Josa-Mutuberría [x], D. Käfer [a], M. Kaur [o], M.N. Kienzle-Focacci [t], J.K. Kim [ap],
J. Kirkby [r], W. Kittel [ad], A. Klimentov [n,aa], A.C. König [ad], M. Kopal [ar], V. Koutsenko [n,aa],
M. Kräber [au], R.W. Kraemer [ah], W. Krenz [a], A. Krüger [at], A. Kunin [n,aa],
P. Ladron de Guevara [x], I. Laktineh [w], G. Landi [q], M. Lebeau [r], A. Lebedev [n],
P. Lebrun [w], P. Lecomte [au], P. Lecoq [r], P. Le Coultre [au], H.J. Lee [h], J.M. Le Goff [r],
R. Leiste [at], P. Levtchenko [ag], C. Li [u], S. Likhoded [at], C.H. Lin [aw], W.T. Lin [aw],
F.L. Linde [b], L. Lista [ab], Z.A. Liu [g], W. Lohmann [at], E. Longo [al], Y.S. Lu [g],
K. Lübelsmeyer [a], C. Luci [al], D. Luckey [n], L. Luminari [al], W. Lustermann [au], W.G. Ma [u],
L. Malgeri [t], A. Malinin [aa], C. Maña [x], D. Mangeol [ad], J. Mans [aj], J.P. Martin [w],
F. Marzano [al], K. Mazumdar [j], R.R. McNeil [f], S. Mele [r,ab], L. Merola [ab], M. Meschini [q],
W.J. Metzger [ad], A. Mihul [l], H. Milcent [r], G. Mirabelli [al], J. Mnich [a], G.B. Mohanty [j],
G.S. Muanza [w], A.J.M. Muijs [b], B. Musicar [an], M. Musy [al], S. Nagy [p], M. Napolitano [ab],
F. Nessi-Tedaldi [au], H. Newman [ae], T. Niessen [a], A. Nisati [al], H. Nowak [at],
R. Ofierzynski [au], G. Organtini [al], C. Palomares [r], D. Pandoulas [a], P. Paolucci [ab],
R. Paramatti [al], G. Passaleva [q], S. Patricelli [ab], T. Paul [k], M. Pauluzzi [af], C. Paus [n],
F. Pauss [au], M. Pedace [al], S. Pensotti [z], D. Perret-Gallix [d], B. Petersen [ad], D. Piccolo [ab],
F. Pierella [i], M. Pioppi [af], P.A. Piroué [aj], E. Pistolesi [z], V. Plyaskin [aa], M. Pohl [t],
V. Pojidaev [q], H. Postema [n], J. Pothier [r], D.O. Prokofiev [ar], D. Prokofiev [ag], J. Quartieri [am],
G. Rahal-Callot [au], M.A. Rahaman [j], P. Raics [p], N. Raja [j], R. Ramelli [au], P.G. Rancoita [z],
R. Ranieri [q], A. Raspereza [at], P. Razis [ac], D. Ren [au], M. Rescigno [al], S. Reucroft [k],
S. Riemann [at], K. Riles [c], B.P. Roe [c], L. Romero [x], A. Rosca [h], S. Rosier-Lees [d], S. Roth [a],
C. Rosenbleck [a], B. Roux [ad], J.A. Rubio [r], G. Ruggiero [q], H. Rykaczewski [au],
A. Sakharov [au], S. Saremi [f], S. Sarkar [al], J. Salicio [r], E. Sanchez [x], M.P. Sanders [ad],
C. Schäfer [r], V. Schegelsky [ag], S. Schmidt-Kaerst [a], D. Schmitz [a], H. Schopper [av],
D.J. Schotanus [ad], G. Schwering [a], C. Sciacca [ab], L. Servoli [af], S. Shevchenko [ae],
N. Shivarov [ao], V. Shoutko [aa,n], E. Shumilov [aa], A. Shvorob [ae], T. Siedenburg [a], D. Son [ap],
P. Spillantini [q], M. Steuer [n], D.P. Stickland [aj], B. Stoyanov [ao], A. Straessner [r],
K. Sudhakar [j], G. Sultanov [ao], L.Z. Sun [u], S. Sushkov [h], H. Suter [au], J.D. Swain [k],
Z. Szillasi [y,3], X.W. Tang [g], P. Tarjan [p], L. Tauscher [e], L. Taylor [k], B. Tellili [w],
D. Teyssier [w], C. Timmermans [ad], Samuel C.C. Ting [n], S.M. Ting [n], S.C. Tonwar [j,r],
J. Tóth [m], C. Tully [aj], K.L. Tung [g], Y. Uchida [n], J. Ulbricht [au], E. Valente [al],
R.T. Van de Walle [ad], V. Veszpremi [y], G. Vesztergombi [m], I. Vetlitsky [aa], D. Vicinanza [am],
G. Viertel [au], S. Villa [ak], M. Vivargent [d], S. Vlachos [e], I. Vodopianov [ag], H. Vogel [ah],
H. Vogt [at], I. Vorobiev [ah,aa], A.A. Vorobyov [ag], M. Wadhwa [e], W. Wallraff [a], M. Wang [n],
X.L. Wang [u], Z.M. Wang [u], M. Weber [a], P. Wienemann [a], H. Wilkens [ad], S.X. Wu [n],
S. Wynhoff [aj], L. Xia [ae], Z.Z. Xu [u], J. Yamamoto [c], B.Z. Yang [u], C.G. Yang [g], H.J. Yang [c],
M. Yang [g], S.C. Yeh [ax], An. Zalite [ag], Yu. Zalite [ag], Z.P. Zhang [u], J. Zhao [u], G.Y. Zhu [g],
R.Y. Zhu [ae], H.L. Zhuang [g], A. Zichichi [i,r,s], G. Zilizi [y,3], B. Zimmermann [au], M. Zöller [a]

[a] *I. Physikalisches Institut, RWTH, D-52056 Aachen, Germany* [1],
III. Physikalisches Institut, RWTH, D-52056 Aachen, Germany [1]
[b] *National Institute for High Energy Physics, NIKHEF, and University of Amsterdam, NL-1009 DB Amsterdam, The Netherlands*
[c] *University of Michigan, Ann Arbor, MI 48109, USA*
[d] *Laboratoire d'Annecy-le-Vieux de Physique des Particules, LAPP, IN2P3-CNRS, BP 110, F-74941 Annecy-le-Vieux Cedex, France*
[e] *Institute of Physics, University of Basel, CH-4056 Basel, Switzerland*
[f] *Louisiana State University, Baton Rouge, LA 70803, USA*
[g] *Institute of High Energy Physics, IHEP, 100039 Beijing, PR China* [6]
[h] *Humboldt University, D-10099 Berlin, Germany* [1]
[i] *University of Bologna, and INFN, Sezione di Bologna, I-40126 Bologna, Italy*
[j] *Tata Institute of Fundamental Research, Mumbai (Bombay) 400 005, India*
[k] *Northeastern University, Boston, MA 02115, USA*
[l] *Institute of Atomic Physics and University of Bucharest, R-76900 Bucharest, Romania*
[m] *Central Research Institute for Physics of the Hungarian Academy of Sciences, H-1525 Budapest 114, Hungary* [2]
[n] *Massachusetts Institute of Technology, Cambridge, MA 02139, USA*
[o] *Panjab University, Chandigarh 160 014, India*
[p] *KLTE-ATOMKI, H-4010 Debrecen, Hungary* [3]
[q] *INFN, Sezione di Firenze, and University of Florence, I-50125 Florence, Italy*
[r] *European Laboratory for Particle Physics, CERN, CH-1211 Geneva 23, Switzerland*
[s] *World Laboratory, FBLJA Project, CH-1211 Geneva 23, Switzerland*
[t] *University of Geneva, CH-1211 Geneva 4, Switzerland*
[u] *Chinese University of Science and Technology, USTC, Hefei, Anhui 230 029, PR China* [6]
[v] *University of Lausanne, CH-1015 Lausanne, Switzerland*
[w] *Institut de Physique Nucléaire de Lyon, IN2P3-CNRS, Université Claude Bernard, F-69622 Villeurbanne, France*
[x] *Centro de Investigaciones Energéticas, Medioambientales y Tecnológicas, CIEMAT, E-28040 Madrid, Spain* [4]
[y] *Florida Institute of Technology, Melbourne, FL 32901, USA*
[z] *INFN, Sezione di Milano, I-20133 Milan, Italy*
[aa] *Institute of Theoretical and Experimental Physics, ITEP, Moscow, Russia*
[ab] *INFN, Sezione di Napoli, and University of Naples, I-80125 Naples, Italy*
[ac] *Department of Physics, University of Cyprus, Nicosia, Cyprus*
[ad] *University of Nijmegen and NIKHEF, NL-6525 ED Nijmegen, The Netherlands*
[ae] *California Institute of Technology, Pasadena, CA 91125, USA*
[af] *INFN, Sezione di Perugia, and Università Degli Studi di Perugia, I-06100 Perugia, Italy*
[ag] *Nuclear Physics Institute, St. Petersburg, Russia*
[ah] *Carnegie Mellon University, Pittsburgh, PA 15213, USA*
[ai] *INFN, Sezione di Napoli, and University of Potenza, I-85100 Potenza, Italy*
[aj] *Princeton University, Princeton, NJ 08544, USA*
[ak] *University of California, Riverside, CA 92521, USA*
[al] *INFN, Sezione di Roma, and University of Rome "La Sapienza", I-00185 Rome, Italy*
[am] *University and INFN, Salerno, I-84100 Salerno, Italy*
[an] *University of California, San Diego, CA 92093, USA*
[ao] *Bulgarian Academy of Sciences, Central Laboratory of Mechatronics and Instrumentation, BU-1113 Sofia, Bulgaria*
[ap] *The Center for High Energy Physics, Kyungpook National University, 702-701 Taegu, South Korea*
[aq] *Utrecht University and NIKHEF, NL-3584 CB Utrecht, The Netherlands*
[ar] *Purdue University, West Lafayette, IN 47907, USA*
[as] *Paul Scherrer Institut, PSI, CH-5232 Villigen, Switzerland*
[at] *DESY, D-15738 Zeuthen, Germany*
[au] *Eidgenössische Technische Hochschule, ETH Zürich, CH-8093 Zürich, Switzerland*
[av] *University of Hamburg, D-22761 Hamburg, Germany*
[aw] *National Central University, Chung-Li, Taiwan, ROC*
[ax] *Department of Physics, National Tsing Hua University, Taiwan, ROC*

Abstract

Bose–Einstein correlations of both neutral and like-sign charged pion pairs are measured in a sample of 2 million hadronic Z decays collected with the L3 detector at LEP. The analysis is performed in the four-momentum difference range 300 MeV $<$ $Q <$ 2 GeV. The radius of the neutral pion source is found to be smaller than that of charged pions. This result is in qualitative agreement with the string fragmentation model. © 2002 Elsevier Science B.V. All rights reserved.

1. Introduction

Bose–Einstein correlations (BEC), between identical bosons, have been extensively studied in hadronic final states produced in e^+e^-, ep, hadron–hadron and heavy-ion interactions [1–3]. The bosons studied are mainly charged pions [4,5]. Only rarely have neutral pions been studied [6,7], and never before in e^+e^- interactions. In this Letter, we report a study of BEC of π^0 pairs in hadronic decays of the Z boson at LEP, and compare them to BEC of pairs of identically charged pions.

BEC manifest themselves as an enhanced production of pairs of identical bosons which are close to one another in phase space. This can be studied in terms of the two-particle correlation function R_2 [4]:

$$R_2(p_1, p_2) = \frac{\rho_{BE}(p_1, p_2)}{\rho_0(p_1, p_2)}, \tag{1}$$

where $\rho_{BE}(p_1, p_2)$ is the two-particle number density for identical bosons with four-momenta p_1 and p_2, subject to Bose–Einstein symmetry. The reference distribution, $\rho_0(p_1, p_2)$, is the same density in the absence of Bose–Einstein symmetry.

Assuming a static spherical boson source with a Gaussian density and a plane wave description of the bosons, $R_2(p_1, p_2)$ is written as [8,9]:

$$R_2(Q) = \mathcal{N}(1 + \alpha Q)\left(1 + \lambda e^{-Q^2 R^2}\right), \tag{2}$$

where $Q^2 = -(p_1 - p_2)^2$ is the square of the four-momentum difference. The parameter R can be interpreted as the size of the boson source in the centre-of-mass system of the boson pair and a measurement of the correlation function R_2 gives access to the source size. The parameter λ is introduced to describe the fraction of effectively interfering pion pairs. In this analysis the normalization factor $\mathcal{N}(1 + \alpha Q)$ is added. It takes into account possible long-range momentum correlations, as well as possible differences in pion multiplicity in the data and reference samples, over the four-momentum difference range studied.

The spherical shape of the boson source assumed here is a simplified picture. High statistics charged pion data at LEP revealed the source to be elongated [4,10]. The present measurement has, however, no sensitivity to the shape of the source of neutral pions, due to its limited statistics.

Several theoretical predictions exist for differences in BEC for pairs of bosons in the pion isospin triplet (π^+, π^-, π^0). From the string model [11] a smaller spatial emission region, i.e., a wider momentum correlation distribution is expected for $\pi^0\pi^0$, than for $\pi^\pm\pi^\pm$. This follows from the break-up of the string into $q\bar{q}$ pairs, which forbids two equally charged pions to lie next to each other on the string, whereas two neutral pions can. The same effect is found when the probabilistic string break-up rule is interpreted as the square of a quantum mechanical amplitude [12,13]. From a quantum statistical approach to Bose–Einstein symmetry [14], a small difference between $\pi^\pm\pi^\pm$ and

$\pi^0\pi^0$ correlation is expected. The size and shape of this difference is predicted to be similar to an expected Bose–Einstein correlation of $\pi^\pm\pi^\mp$ pairs. It is theoretically uncertain whether BEC between unlike sign pions are also to be expected on the ground of isospin invariance [15].

The main purpose of this Letter is to measure the difference in size of the emission region of neutral and charged pions. In order to minimize systematic uncertainties on this difference, the procedures followed for the charged pions are kept as close as possible to those for the neutral pions.

2. Data and Monte Carlo samples

For this analysis, data collected with the L3 detector [16] during the 1994 and 1995 LEP runs are used. The analysis is based mainly on measurements from the high resolution electromagnetic calorimeter and from the central tracking device. The data sample corresponds to an integrated luminosity of about 78 pb^{-1} at centre-of-mass energies around $\sqrt{s} = 91.2$ GeV. From this sample, about 2 million hadronic events are selected, using energy deposits in the electromagnetic and hadronic calorimeters [17].

The JETSET generator [18] is used to study the detector response to hadronic events. Parameters of the generator are tuned to give a good description of event and jet shapes of hadronic events measured in L3. The effects of Bose–Einstein symmetry are simulated with the Luboei routine [19]. The routine has two parameters, which have been chosen to obtain a reasonable description of L3 data. This *ad-hoc* model shifts boson momenta after the hadronization phase in such a way that the correlation function $R_2(Q)$ for identical bosons is proportional to a constant plus a Gaussian as in Eq. (2). The generated events are passed through a full detector simulation [20] and are reconstructed and subjected to the same analysis procedure as the data. This Monte Carlo sample (JETSET-BE) contains about 7 million events. A control sample (JETSET-NOBE) is also generated with JETSET but it has Luboei switched off and the generator parameters returned. Significant differences are found in the tuned parameters in the two cases. The number of events in the control sample is approximately 2 million. Unless stated otherwise,

the JETSET-BE sample is used throughout this Letter.

3. Neutral pion selection

Neutral pions in hadronic events are reconstructed from photon pairs. Photon candidates are identified in the electromagnetic calorimeter as a cluster of at least two adjacent crystals. The clusters are required to be located in the central region of the detector, $|\cos(\theta_{\text{cluster}})| < 0.73$, and to be in the energy range 100 MeV $< E_{\text{cluster}} < 6$ GeV. Above 6 GeV, the two photons from a π^0 decay can no longer be distinguished as two separate clusters.

Discrimination of clusters originating from photons or electrons from those due to other particles is based on the distribution of the energy over the crystals of the cluster. A good photon discrimination is achieved with a neural network based on this energy distribution [21]. To reject clusters due to charged particles, a minimum distance between the cluster and the extrapolation of the closest track of 30 mm is required. This corresponds to 1.5 times the size of the front face of a crystal.

Pairs of photon candidates within an event are used to reconstruct π^0's. The distribution of invariant mass of photon pairs shows a peak around the π^0 mass, above a smooth background. These two components are extracted by a fit to the mass spectrum. The background is described by a Chebyshev polynomial of third order, f_{bg}. The π^0 peak is parameterized by a Gaussian function with exponential tails, which is continuous, and smooth in the first derivative:

$$f_\pi(m_{\gamma\gamma}) = \begin{cases} \exp\left(\frac{\alpha^2}{2}\right)\exp\left(\frac{\alpha(m_{\gamma\gamma}-m_\pi)}{\sigma}\right) \\ \quad \text{if } m_{\gamma\gamma} - m_\pi < -\alpha\sigma, \\ \exp\left(-\frac{(m_{\gamma\gamma}-m_\pi)^2}{2\sigma^2}\right) \\ \quad \text{if } \beta\sigma \geqslant m_{\gamma\gamma} - m_\pi \geqslant -\alpha\sigma, \\ \exp\left(\frac{\beta^2}{2}\right)\exp\left(-\frac{\beta(m_{\gamma\gamma}-m_\pi)}{\sigma}\right) \\ \quad \text{if } m_{\gamma\gamma} - m_\pi > \beta\sigma. \end{cases} \tag{3}$$

Here, $m_{\gamma\gamma}$ is the two-photon invariant mass, m_π indicates the peak position, and σ is the width of the Gaussian peak. The parameters α and β determine the values of $m_{\gamma\gamma}$ where the Gaussian changes into an exponential. The exponential tail at low mass is needed to describe the presence of converted photons

in cluster pairs. If a photon converts, e.g., in the outer wall of the tracker, it can still be selected as a photon, although some of the original photon energy is lost. The high mass tail accounts for an overestimate of the cluster energy due to another cluster nearby.

An example of the fit result is given in Fig. 1. The sum of the two functions f_{bg} and f_π describes the distribution well. Also, the shape and the size of the π^0 peak in the data and Monte Carlo agree. The mass resolution as determined from the fit is about 7.4 MeV.

The photon pair is then selected as a π^0 candidate if it has an energy 200 MeV $< E_{\gamma\gamma} <$ 6 GeV. For a mass window 120 MeV $< m_{\gamma\gamma} <$ 150 MeV, a total of 1.3 million π^0's is selected in data. The π^0 purity of the candidate sample is of the order of 54% and the π^0 selection efficiency is approximately 17%. About half of the background is combinatorial, i.e., photons from different π^0's. The other half consists of pairs where one or both of the photons do not come from a π^0 decay.
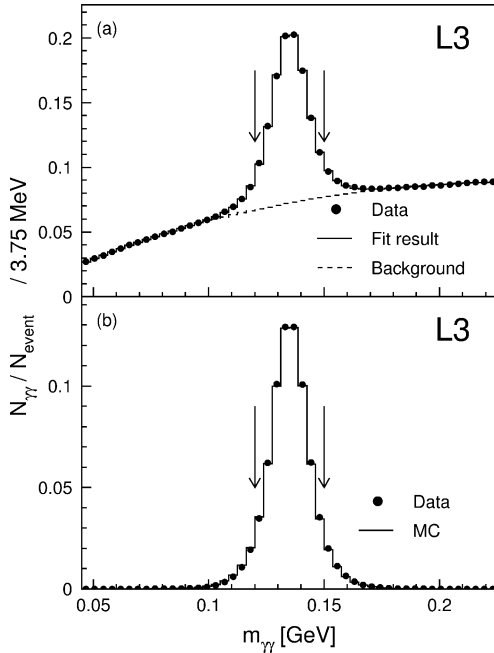

Fig. 1. Distribution of (a) the two-photon invariant mass $m_{\gamma\gamma}$ for data together with the fit result and (b) the π^0 signal as obtained from fits to data and to Monte Carlo. The arrows indicate the mass selection window.

4. Charged pion selection

Charged pions are detected as tracks in the central tracker. They are selected in the same kinematic range as neutral pions: $|\cos(\theta_{track})| < 0.73$ and 200 MeV $< E_{track} <$ 6 GeV, where the energy is calculated from the track momentum, assuming the $\pi^\pm$ mass. In addition, at least 35 out of 62 possible wire hits are required in the track fit, and the number of wires between the first and the last must be at least 50. Furthermore, the track must have at least one hit in the inner part of the tracker, and the distance of closest approach to the e^+e^- vertex in the plane transverse to the beam is required to be less than 5 mm. Finally, a high resolution measurement of the polar angle is demanded. Charged pions are analyzed in the 1995 data only, in which 4.1 million tracks are selected.

5. Pion pair analysis

5.1. Neutral pions

After the neutral pion selection, π^0 candidates within an event are paired, requiring that no cluster is common to the two candidates, and their four-momentum difference Q is calculated. The $\pi^0\pi^0$ component of the Q distribution is estimated by a fit to the two-dimensional mass spectrum for every bin in Q. An example of these mass distributions is shown in Fig. 2(a), for the bin $0.48 < Q < 0.52$ GeV. The various contributions are clearly visible: non-π^0 pairs give the smooth background, π^0 with non-π^0 pairs give the two "ridges" in the π^0 peak regions, π^0 pairs give part of the peak in the centre of the plot, the other part being caused by the sum of the π^0 with non-π^0 ridges.

This two-dimensional distribution is derived from the product of two one-dimensional mass distributions [21]:

$$
\begin{aligned}
f_{2d}(m_1, m_2) &= A_{\pi\pi} f_\pi(m_1) f_\pi(m_2) \\
&\quad + A_{\pi bg}\big[f_\pi(m_1) f_{bg}(m_2) + f_{bg}(m_1) f_\pi(m_2) \big] \\
&\quad + A_{bgbg} f_{bgbg}(m_1, m_2),
\end{aligned} \tag{4}
$$

where the first term describes the $\pi^0\pi^0$ part, the second term describes the π^0 with non-π^0 pair ridges

and the third term is the non-π^0 pair background. The number of π^0 pairs in the mass window 120 MeV $<$ $m_{1,2} <$ 150 MeV is related to the parameter $A_{\pi\pi}$. The functions f_π and f_{bg} have the same functional form as described before, f_{bgbg} follows from the product of two Chebyshev polynomials of third order and is required to be symmetric in the two masses. All 18 parameters of f_{2d} are left free in the fit.

The result of a binned maximum likelihood fit for the mass distribution in Fig. 2(a) is shown in Figs. 2(b)–(d). In this representative example, the χ^2 is 4737 for 4606 degrees of freedom, which corresponds to a 9% confidence level.

Fig. 3(a) presents the Q distribution for π^0 pairs in the mass window 120 MeV $< m_{1,2} <$ 150 MeV,

obtained from the values of the parameter $A_{\pi\pi}$ from two-dimensional mass fits of Eq. (4) to both data and Monte Carlo. Some deviations between data and Monte Carlo are caused by the imperfect modeling of BEC. The efficiency to select a π^0 pair in an event ranges from about 1% at $Q = 300$ MeV to 4% at $Q = 2$ GeV.

Bins in Q below 300 MeV are not used for the rest of the analysis for two reasons. First, the efficiency estimate depends strongly on the BEC modeling in the generator, in the region of small Q. This occurs because the BEC modeling moves identical pions closer together, which lowers the detection efficiency. Secondly, the four-momentum difference of any pair of π^0's from $\eta \to \pi^0\pi^0\pi^0$ decays is kinematically
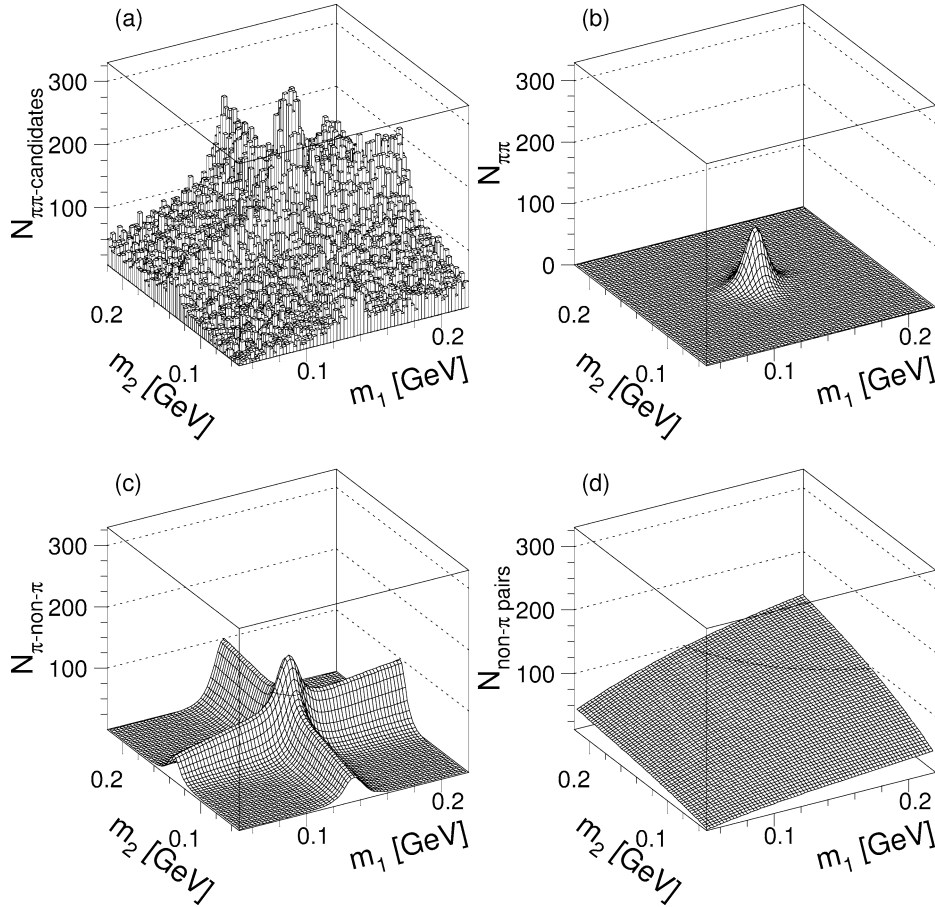

Fig. 2. (a) Two-dimensional distribution of the mass of π^0 pair candidates with a four-momentum difference in the range $0.48 < Q < 0.52$ GeV, in bins of 2.5×2.5 MeV^2. Result of the fit for (b) π^0 pairs, (c) π^0 with non-π^0 pairs, (d) non-π^0 pairs.

constrained to have $Q < 311.7$ MeV, and in that Q-range, more than 20% of all π^0 pairs originate from this decay. A rejection of the small Q region thus avoids systematic uncertainties due to the simulation of the η multiplicity.

5.2. Charged pions

The distribution of four-momentum difference of equally charged pion pairs is obtained by calculating Q for pairs of tracks selected within an event and with the same charge. This raw $\pi^\pm\pi^\pm$ spectrum is corrected bin-by-bin for both pion purity and efficiency using the Monte Carlo simulation. The uncorrected distribution is shown in Fig. 3(b). Compared to the $\pi^0\pi^0$ case, smaller deviations are observed between the raw spectrum in data and Monte Carlo. These deviations are due to the imperfect modeling of BEC in the Monte Carlo.
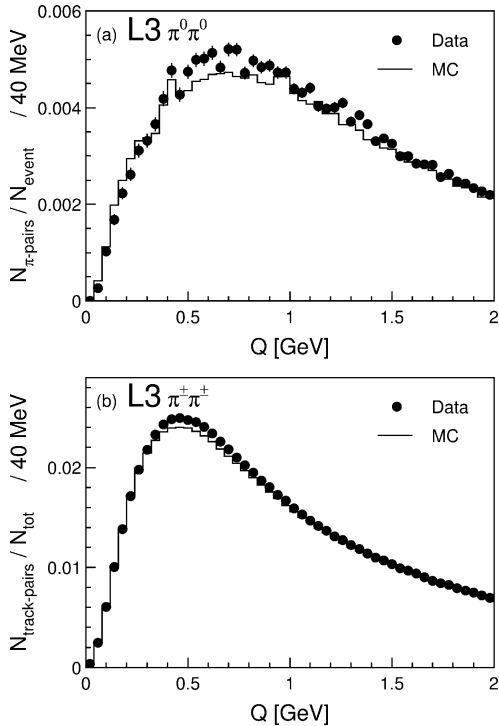

Fig. 3. Data and Monte Carlo distribution of the four-momentum difference of (a) pairs of π^0's, as obtained from fits of Eq. (4), and (b) pairs of $\pi^\pm$ candidates.

6. Results

6.1. Neutral pions

To obtain the final correlation function $R_2(Q)$, the Q distribution of π^0 pairs in the data, Fig. 3(a), is corrected for selection efficiencies. The efficiency is defined as the number of selected π^0 pairs in Monte Carlo events (JETSET-BE) divided by the number of generated π^0 pairs in the same events, where the generated pions have to be in the same kinematic range as the selected pions. This definition includes an acceptance correction for those π^0's which cannot be selected kinematically. In this way, the correlations of π^0 pairs can directly be compared to those of charged pion pairs. The reference distribution $\rho_0(Q)$ is calculated from a JETSET-NOBE sample at generator level, where pions are taken in the same kinematic range as in the definition of the selection efficiency. We choose this reference distribution rather than the distribution for $\pi^\pm\pi^\mp$ because of the uncertainty concerning BEC between unlike sign pions mentioned in the introduction. The correlation distribution $R_2(Q)$ is then the ratio of the corrected data spectrum to the reference spectrum.

The distribution of $R_2(Q)$ is displayed in Fig. 4(a). An enhancement at low Q values, expected from Bose–Einstein symmetry, is clearly visible. The function $R_2(Q)$ from Eq. (2) is fitted to this ratio in the interval 300 MeV $< Q < 2$ GeV. Extending the fit to lower values of Q results in consistent values of the parameters but with much larger systematic uncertainties. The overall normalization $\mathcal{N}$ is determined from the integrals of $R_2(Q)$ and the fit function; the only free parameters are λ, R and α. In this fit, the χ^2 is 46.1 for 40 degrees of freedom, corresponding to a 23% confidence level.

The systematic uncertainty on the result due to the π^0 selection is determined by varying the photon selection cuts and by changing the size of the π^0 mass window by ± 10 MeV. The $\pi^0\pi^0$ mass fit of Eq. (4) is tested by varying the fit range by ± 12.5 MeV. The uncertainty due to the modeling of Bose–Einstein correlations in the Monte Carlo generator is taken into account by using the control sample JETSET-NOBE in the efficiency correction procedure. In addition, the influence on the final result of the agreement between data and Monte Carlo of

Table 1
Systematic uncertainties on λ, R and α for the $\pi^0\pi^0$ data sample

Source	$\Delta\lambda$	ΔR (fm)	$\Delta\alpha$
Photon selection	0.020	0.052	0.009
Mass window	0.011	0.008	0.007
2D fit range	0.056	0.019	0.036
MC modeling	0.037	0.035	0.020
Data-MC agreement	0.012	0.018	0.034
Q-binning	0.004	0.013	0.003
Total	0.072	0.070	0.055

Table 2
Systematic uncertainties on λ, R and α for the $\pi^\pm\pi^\pm$ data sample

Source	$\Delta\lambda$	ΔR (fm)	$\Delta\alpha$
Track selection	0.011	0.009	0.009
MC modeling	0.022	0.003	0.002
Q-binning	0.001	0.001	0.001
Total	0.025	0.010	0.009

distributions relevant to the photon and π^0 selection, such as neural network output and energy and polar angle of π^0's, is studied. Finally, the binning in Q is varied. The systematic uncertainty on the result due to each of the sources, is assigned as half the maximum deviation. A summary is given in Table 1. The total systematic uncertainty is calculated as the quadratic sum of these uncertainties.

6.2. Charged pions

The final correlation function $R_2(Q)$ for $\pi^\pm\pi^\pm$ is calculated in a similar way as that for $\pi^0\pi^0$. The $\pi^\pm\pi^\pm$ data distribution, Fig. 3(b), is corrected for purity and efficiency. As for $\pi^0\pi^0$, the efficiency is calculated for generated pions in the same kinematic range as the selected pions. The reference distribution $\rho_0(Q)$ and the correlation distribution $R_2(Q)$ are obtained in the same way as for $\pi^0\pi^0$.

The correlation function for $\pi^\pm\pi^\pm$ is shown in Fig. 4(b). Due to the higher selection efficiency for charged pions as compared to neutral pions, the significance of the low Q value enhancement is much larger. As for $\pi^0\pi^0$, the function defined in Eq. (2) is fitted to the final distribution. In this fit, the χ^2 is 42.6 for 40 degrees of freedom, corresponding to a 36% confidence level.

The systematic uncertainty on the result due to the track selection is determined by varying the requirements on number of hits, distance of closest approach and polar angle determination. As in the $\pi^0\pi^0$ case, the uncertainty on the modeling of Bose–Einstein cor-

relations in the Monte Carlo generator is obtained by using the control sample JETSET-NOBE in the analysis. Finally, the binning in Q is varied. The systematic uncertainties are attributed as in the $\pi^0\pi^0$ case, and are summarized in Table 2. The total systematic uncertainty is calculated as the quadratic sum of these uncertainties.
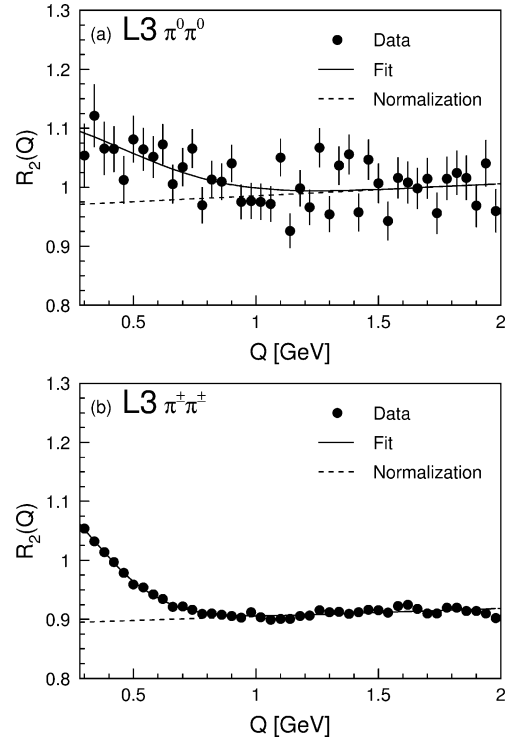

Fig. 4. Distribution of $R_2(Q)$ for (a) $\pi^0\pi^0$ and (b) $\pi^\pm\pi^\pm$, and results of the fits. The points indicate the data, the full line corresponds to the fit result and the dashed line is the normalization factor $\mathcal{N}(1 + \alpha Q)$.

Table 3
Values for λ, R and α, for both the $\pi^0\pi^0$ and the $\pi^\pm\pi^\pm$ data samples. The first uncertainty is statistical, the second systematic

Sample	λ	R (fm)	α
$\pi^0\pi^0$	$0.155 \pm 0.054 \pm 0.072$	$0.309 \pm 0.074 \pm 0.070$	$0.021 \pm 0.034 \pm 0.055$
$\pi^\pm\pi^\pm$	$0.286 \pm 0.008 \pm 0.025$	$0.459 \pm 0.010 \pm 0.010$	$0.015 \pm 0.003 \pm 0.009$

6.3. Comparison

The final values for the strength of the correlation λ and the corresponding radii of the boson sources R are given in Table 3.

Due to the lower efficiency of the $\pi^0\pi^0$ selection, the statistical uncertainty on the $\pi^0\pi^0$ result is larger than the statistical uncertainty on the $\pi^\pm\pi^\pm$ result. Within these uncertainties, the data indicate both a weaker correlation and a smaller source radius for $\pi^0\pi^0$. The weakness of the $\pi^0\pi^0$ correlation can be partly explained by the bigger contribution of resonance decays to the Q spectrum. The difference of the source sizes is

$$R_{\pm\pm} - R_{00} = 0.150 \pm 0.075 \text{ (stat.)}$$
$$\pm 0.068 \text{ (syst.) fm,} \qquad (5)$$

where $R_{\pm\pm}$ and R_{00} indicate the value of R for $\pi^\pm\pi^\pm$ and $\pi^0\pi^0$, respectively. In this difference, the systematic uncertainties due to the modeling of Bose–Einstein correlations and the binning in Q are taken to be correlated between the two samples. The smaller radius found for $\pi^0\pi^0$ is in qualitative agreement with the predictions of the string model.

Acknowledgements

References

[1] G. Goldhaber et al., Phys. Rev. Lett. 3 (1959) 181.
[2] D.H. Boal, C.K. Gelbke, B.K. Jennings, Rev. Mod. Phys. 62 (1990) 553.
[3] G. Baym, Acta Phys. Pol. B 29 (1998) 1839.
[4] L3 Collaboration, M. Acciarri et al., Phys. Lett. B 458 (1999) 517.
[5] ALEPH Collaboration, D. Decamp et al., Z. Phys. C 54 (1992) 75;
DELPHI Collaboration, P. Abreu et al., Phys. Lett. B 286 (1992) 201;
OPAL Collaboration, G. Alexander et al., Z. Phys. C 72 (1996) 389.
[6] K. Eskreys, Acta Phys. Pol. 36 (1969) 237.
[7] V.G. Grishin et al., Sov. J. Nucl. Phys. 47 (1988) 278.
[8] G. Goldhaber, S. Goldhaber, W. Lee, A. Pais, Phys. Rev. 120 (1960) 300.
[9] M. Deutschmann et al., Nucl. Phys. B 204 (1982) 333.
[10] DELPHI Collaboration, P. Abreu et al., Phys. Lett. B 471 (2000) 460;
OPAL Collaboration, G. Abbiendi et al., Eur. Phys. J. C 16 (2000) 423.
[11] B. Andersson et al., Phys. Rep. 97 (1983) 31.
[12] B. Andersson, W. Hofmann, Phys. Lett. B 169 (1986) 364.
[13] B. Andersson, M. Ringnér, Nucl. Phys. B 513 (1998) 627.
[14] I.V. Andreev, M. Plümer, R.M. Weiner, Phys. Rev. Lett. 67 (1991) 3475.
[15] M. Suzuki, Phys. Rev. D 35 (1987) 3359;
M.G. Bowler, Phys. Lett. B 197 (1987) 443;
G. Alexander, H.J. Lipkin, Phys. Lett. B 456 (1999) 270.
[16] L3 Collaboration, B. Adeva et al., Nucl. Instrum. Methods A 289 (1990) 35;
M. Acciarri et al., Nucl. Instrum. Methods A 351 (1994) 300;
A. Adam et al., Nucl. Instrum. Methods A 383 (1996) 342;
I.C. Brock et al., Nucl. Instrum. Methods A 381 (1996) 236;
M. Chemarin et al., Nucl. Instrum. Methods A 349 (1994) 345.
[17] L3 Collaboration, M. Acciarri et al., Eur. Phys. J. C 16 (2000) 1.
[18] T. Sjöstrand, Comput. Phys. Commun. 82 (1994) 74.
[19] L. Lönnblad, T. Sjöstrand, Phys. Lett. B 351 (1995) 293.
[20] The L3 detector simulation is based on GEANT Version 3.15;
See R. Brun et al., GEANT 3, CERN DD/EE/84-1 (1984), revised 1987;
The GHEISHA program (H. Fesefeldt, RWTH Aachen Report PITHA 85/02 (1985), is used to simulate hadronic interactions.
[21] M.P. Sanders, Ph.D. Thesis, University of Nijmegen, 2002.